

Mesenchymal Stem Cells Induce Epithelial to Mesenchymal Transition in Colon Cancer Cells through Direct Cell-to-Cell Contact¹



Hidehiko Takigawa^{*}, Yasuhiko Kitadai[†], Kei Shinagawa[‡], Ryo Yuge[§], Yukihito Higashi[¶], Shinji Tanaka[§], Wataru Yasui[#] and Kazuaki Chayama^{*,**,††}

^{*}Department of Gastroenterology and Metabolism, Hiroshima University, Hiroshima, Japan; [†]Department of Health and Science, Prefectural University of Hiroshima, Hiroshima, Japan; [‡]Central Clinic, Hiroshima, Japan; [§]Department of Endoscopy and Medicine, Hiroshima University, Hiroshima, Japan; [¶]Department of Cardiovascular Physiology and Medicine, Hiroshima University, Hiroshima, Japan; [#]Department of Molecular Pathology, Hiroshima University, Hiroshima, Japan; ^{**}Liver Research Project Center, Hiroshima University, Hiroshima, Japan.; ^{††}Laboratory for Digestive Diseases, RIKEN Center for Integrative Medical Sciences, Hiroshima, Japan

Abstract

We previously reported that in an orthotopic nude mouse model of human colon cancer, bone marrow–derived mesenchymal stem cells (MSCs) migrated to the tumor stroma and promoted tumor growth and metastasis. Here, we evaluated the proliferation and migration ability of cancer cells cocultured with MSCs to elucidate the mechanism of interaction between cancer cells and MSCs. Proliferation and migration of cancer cells increased following direct coculture with MSCs but not following indirect coculture. Thus, we hypothesized that direct contact between cancer cells and MSCs was important. We performed a microarray analysis of gene expression in KM12SM colon cancer cells directly cocultured with MSCs. Expression of epithelial-mesenchymal transition (EMT)–related genes such as fibronectin (*FN*), *SPARC*, and galectin 1 was increased by direct coculture with MSCs. We also confirmed the upregulation of these genes with real-time polymerase chain reaction. Gene expression was not elevated in cancer cells indirectly cocultured with MSCs. Among the EMT-related genes upregulated by direct coculture with MSCs, we examined the immune localization of FN, a well-known EMT marker. In coculture assay in chamber slides, expression of FN was seen only at the edges of cancer clusters where cancer cells directly contacted MSCs. FN expression in cancer cells increased at the tumor periphery and invasive edge in orthotopic nude mouse tumors and human colon cancer tissues. These results suggest that MSCs induce EMT in colon cancer cells via direct cell-to-cell contact and may play an important role in colon cancer metastasis.

Neoplasia (2017) 19, 429–438

Introduction

Colorectal cancer (CRC) is the third most common cancer and a major cause of mortality worldwide [1]. Many studies have indicated that tumor growth and metastasis are determined by both tumor cells and stromal cells. The stroma constitutes a large percentage of most solid tumors, and tumor-stromal cell interactions contribute to tumor growth and metastasis [2,3]. Of the constituents of the tumor stroma, it has become clear that activated fibroblasts, known as

Address all correspondence to: Yasuhiko Kitadai, 1-1-71 Ujinahigashi, Minami-ku, Hiroshima 734-8558, Japan. E-mail: kitadai@pu-hiroshima.ac.jp

¹ Funding Information: Supported in part by PUH Research Grant Program and grants-in-aid for cancer research from the Ministry of Education, Culture, Science, Sports, and Technology of Japan.

Received 15 January 2017; Revised 15 February 2017; Accepted 21 February 2017

© 2017 The Authors. Published by Elsevier Inc. on behalf of Neoplasia Press, Inc. This is an open access article under the CC BY-NC-ND license (<http://creativecommons.org/licenses/by-nc-nd/4.0/>). 1476-5586

<http://dx.doi.org/10.1016/j.neo.2017.02.010>

carcinoma-associated fibroblasts (CAFs), promote tumor growth and metastasis [4–6].

We previously reported that mesenchymal stem cells (MSCs) incorporated into the stroma of primary and metastatic tumors expressed α -smooth muscle actin and platelet-derived growth factor receptor- β as CAF markers. KM12SM cells recruited MSCs, and MSCs stimulated migration and invasion of tumor cells. MSCs migrate and differentiate into CAFs in the tumor stroma [7]. Coimplantation of KM12SM cells with MSCs into the cecal walls of nude mice produced tumors with abundant stromal components and promoted tumor growth and lymph node metastasis by enhancing angiogenesis, migration, and invasion and by inhibiting apoptosis of tumor cells [8].

MSCs may provide delivery vehicles for antitumor biological agents because of their ability to migrate to tumors [9]. A number of antitumor genes have been engineered into MSCs and have demonstrated antitumor effects on various cancer models [10–18]. However, there are potential concerns in using MSCs as delivery vehicles; we understand little about the fate of this cell population *in vivo* [19,20], and there is a possibility that MSCs themselves might enhance or initiate tumor growth [21–23].

It has been shown that MSCs can promote tumor proliferation and expression of an epithelial-mesenchymal transition (EMT) phenotype in several cancer cells via expression of proteins including TWIST, MMP, WNT5A, and TGF- β type I receptor [24–26], many of which act in a paracrine manner. Previous reports have suggested that paracrine factors expressed by MSCs affect cancer cells. However, this does not necessarily mean that the interaction between cancer cells and MSCs is paracrine in nature. Whereas some reports have indicated that the interaction between cancer cells and MSCs is regulated via paracrine signaling [27], other reports have indicated that the interaction may be regulated via juxtacrine signaling [28]. The mechanism of secretion and interaction between cancer cells and MSCs therefore remains to be elucidated.

Thus, in this study, we examined tumor-MSC interactions via direct and indirect coculture of KM12SM colon cancer cells and bone marrow-derived MSCs using cDNA microarray analysis. Direct coculture of MSCs increased proliferation and migration of cancer cells and expression of EMT-related genes such as fibronectin (FN). In addition, coimplantation of MSCs with cancer cells increased the expression of FN at the edges of orthotopic colon cancer tumors, where the tumor stroma directly contacted cancer cells. Expression of FN was correlated with invasion depth of human colorectal carcinoma based on analysis of surgical specimens. Taken together, we found that MSCs promote the progression of colon tumors by inducing EMT through direct cell-to-cell contact.

Material and Methods

Human Colon Carcinoma Cell Line and Culture Conditions

The human colon cancer cell line KM12SM [29] was kindly donated by Dr. Isaiah J. Fidler (University of Texas, Houston, TX). The KM12SM cell line is a highly metastatic clonal cell line selected from the parental KM12C cell line. Cells were maintained in Dulbecco's modified Eagle's medium (DMEM) with 10% fetal bovine serum (FBS; Sigma-Aldrich, St. Louis, MO) and a penicillin-streptomycin mixture. Cultures were maintained for no longer than 12 weeks after recovery of cells from frozen stock.

Transfection and Selection of Stable KM12SM Cells Expressing Green Fluorescent Protein

Green fluorescent protein (GFP) and puromycin resistance genes were transfected into KM12SM colon cancer cells using copGFP Control Lentiviral Particles (sc-108,084; Santa Cruz Biotechnology) according to the manufacturer's protocol. Cells were maintained in complete medium containing puromycin.

Isolation and Culture of Human MSCs

Human MSCs were obtained from the iliac crest and plated in a dish with DMEM supplemented with 10% FBS, L-glutamine, and a penicillin-streptomycin mixture according to a protocol approved by the Ethics Committee of Hiroshima University Graduate School of Medicine, as described previously [30]. Nonadherent cells were removed after 72 hours, and adherent cells were detached from the plates and subcultured every 4 to 5 days in fresh medium supplemented with 1 ng/ml of fibroblast growth factor-2 [31]. Aliquots from passages 3 to 5 were frozen in liquid nitrogen for future use.

Characterization of Human MSCs In Vitro

In culture medium, MSCs formed a monolayer of adherent cells and appeared as long, spindle-shaped fibroblastic cells. Capacity for chondrogenic, adipogenic, and osteogenic differentiation was confirmed with the use of a Human Mesenchymal Stem Cell Functional Identification Kit (R&D Systems, Minneapolis, MN). Cell surface antigens on the cells were analyzed by fluorescence-activated cell sorting (FACS), and we confirmed that the cells were positive for CD29, CD44, CD73, CD90, CD105, CD166, and MHC-DR but negative for CD14, CD34, and Flk-1, as described previously [30].

Preparation of Conditioned Medium

For preparation of conditioned medium from MSCs, cells were seeded on 100-mm cell culture dishes and cultured in fresh medium supplemented with 10% FBS, L-glutamine, a penicillin-streptomycin mixture, and 1 ng/ml of fibroblast growth factor-2 until reaching confluence. Cells were briefly rinsed twice with phosphate-buffered saline (PBS), followed by incubation with 10 ml of medium supplemented with 0.5% FBS for 48 hours prior to collection of culture medium. Culture supernatants were centrifuged at 700 \times g for 10 minutes for removal of cell debris.

Evaluation of Cell Proliferation and Motility In Vitro

KM12SM colon cancer cell lines (6×10^4 cells per well) were seeded into 24-well plates (Essen ImageLock; Essen Bioscience, Ann Arbor, MI) containing DMEM supplemented with 0.5% FBS. KM12SM cells were cultured alone, with MSCs (6×10^4 cells per well), or with MSC-conditioned medium (MSC-CM). Growth curves were generated from a bright-field image obtained using a label-free, high-content time-lapse assay system (IncuCyte Zoom; Essen Bioscience) that automatically expresses cell confluence as a percentage over a 4-day period. All experiments were performed in triplicate.

Cell migration was assessed by performing a scratch wound assay. KM12SM colon cancer cells (1×10^5 cells per well) were seeded in 100 μ g/l Matrigel-coated (BD Biosciences, Bedford, MA) 96-well plates (Essen ImageLock) containing DMEM supplemented with 0.5% FBS. Cancer cells were cultured alone, with MSCs (1×10^5 cells per well), or with MSC-CM. Use of ImageLock 96-well plates allows wound images to be taken automatically at exact locations

using IncuCyte software. Confluent cell layers were scratched using a 96-pin wound maker provided by IncuCyte [32]. After inducing wounds, cells were washed twice with PBS to remove detached cells, and wound images were acquired automatically every 3 hours over a 2-day period. Relative wound density was analyzed automatically by IncuCyte software. All experiments were performed in triplicate.

FACS-Based Isolation of KM12SM Cells from Direct MSC Coculture

KM12SM cells were red-labeled with PKH26-GL (Sigma-Aldrich) according to the manufacturer's protocol. PKH26-GL-labeled KM12SM cells were seeded onto 100-mm dishes at a density of 1×10^4 per well in DMEM supplemented with 0.5% FBS with and without 8×10^5 MSCs. After 24 hours of incubation, cells were subjected to FACS analysis to yield PKH26-GL-positive KM12SM cells according to a standard protocol. RNA samples for microarray analysis were extracted from KM12SM cell culture with an RNeasy Kit (Qiagen, Valencia, CA) according to the manufacturer's instructions.

Isolation of KM12SM Cells from Indirect Coculture

KM12SM cells were seeded onto 100-mm dishes at a density of 1×10^4 per well in DMEM supplemented with 0.5% FBS with and without MSC-CM. After 24 hours of incubation, RNA samples for microarray analysis were extracted from KM12SM cell culture with an RNeasy Kit (Qiagen) according to the manufacturer's instructions.

Microarray Analysis

For oligo DNA microarray analysis, RNA samples were extracted from KM12SM cells cultured alone and KM12SM cells directly cocultured with MSCs. Isolation of KM12SM cells was performed as described above. RNA samples from KM12SM cells in monolayer culture without MSCs represented the control condition. For microarray analysis, a 3D-Gene Human Oligo Chip 25k (Toray Industries Inc., Tokyo, Japan) was used. For efficient hybridization, this microarray is constructed in three dimensions, with a well as the space between the probes and cylinder stems and with 70-mer oligonucleotide probes on the top. Total RNA was labeled with Cy3 (KM12SM cells cultured alone) or Cy5 (KM12SM cells with MSCs) using the Amino Allyl MessageAMP II aRNA Amplification Kit (Applied Biosystems, Carlsbad, CA). Cy3- or Cy5-labeled aRNA pools were mixed with hybridization buffer and hybridized for 16 hours. Hybridization was performed using the supplier's protocols (www.3d-gene.com). Hybridization signals were obtained using 3D-Gene Scanner (Toray Industries Inc.) and processed by 3D-Gene Extraction (Toray Industries Inc.). Detected signals for each gene were normalized using a global normalization method (Cy5/Cy3 ratio median = 1). Genes with Cy5/Cy3 normalized ratios greater than 2.0 or less than 0.5 were defined as up- or downregulated genes, respectively.

Quantitative Reverse Transcription Polymerase Chain Reaction

Total RNA was extracted from gastric cancer cell lines and biopsy specimens with an RNeasy Kit (Qiagen) according to the manufacturer's instructions. cDNA was synthesized from 1 μ g total RNA with a first-strand cDNA synthesis kit (Amersham Biosciences, Piscataway, NJ). After reverse transcription of RNA into cDNA, quantitative reverse transcription polymerase chain reaction (qRT-PCR) was

performed with a LightCycler FastStart DNA Master SYBR Green I Kit (Roche Diagnostics, Basel, Switzerland) according to the manufacturer's recommended protocol. Reactions were carried out in triplicate. To correct for differences in both RNA quality and quantity between samples, expression values were reported as log 2 ratios, normalized to glyceraldehyde-3-phosphate dehydrogenase (*GAPDH*), and mean-centered. Primers for PCR were designed with specific primer analysis software (Primer Designer; Scientific and Educational Software, Cary, NC), and sequence specificity was confirmed by FASTA (European Molecular Biology Laboratory Database, Heidelberg, Germany). Primer sequences are provided in Table 1.

Animals and Transplantation of Tumor Cells

Animal experiments were performed previously [33]. Briefly, female athymic BALB/c nude mice were obtained from Charles River Japan (Tokyo, Japan). The mice were maintained under specific pathogen-free conditions and used at 8 weeks old. Study was carried out after permission was granted by the Committee on Animal Experimentation of Hiroshima University. To produce cecal tumors, KM12SM cells alone (0.5×10^6) or KM12SM cells mixed with MSCs in a ratio of 1:2 (0.5×10^6 : 1.0×10^6 KM12SM:MSCs) in 50 μ l of Hanks' balanced salt solution were injected into the cecal walls of nude mice under a dissecting microscope as described previously [4]. Six weeks after intracecal transplantation of these cells, surviving mice were sacrificed. To evaluate the migration and colocalization of MSCs in orthotopic tumors, 1.0×10^6 KM12SM cells were transplanted into the cecal walls of three mice on day 0. Three weeks after tumor cell transplantation (on day 21), each mouse underwent injection of 1.0×10^6 PKH26-GL-labeled MSCs in 200 μ l of Hanks' balanced salt solution into the tail vein. One week after this injection (on day 28), the mice were killed and necropsied. Tumor tissue was embedded in OCT Compound, rapidly frozen in liquid nitrogen, and stored at -80°C . For this study, we performed only additional analyses using the frozen sections obtained in the previous study [33].

Immunohistochemical Staining of Formalin-Fixed Sections

Formalin-fixed, paraffin-embedded tissues cut into serial 4-mm sections were used for immunohistochemistry. The procedures for immunohistochemical detection of FN have been described previously [34].

Table 1. Primers Used in This Study for Quantitative Real-Time PCR

Gene Symbol	Direction	Sequence (5'-3')	Product Size (bp)
<i>MT1E</i>	Forward	tcttcaagtgcacaagatg	222
	Reverse	cagcaaatggcctcagtggtg	
<i>MT2A</i>	Forward	gcaaatgcaagagtgcaaa	222
	Reverse	atagcaaacggcctcaggtca	
<i>SPARC</i>	Forward	atgaggccctggatctctt	192
	Reverse	ctcttcggttctcctctgcac	
<i>FSTL1</i>	Forward	gcacaggcaactgtgagaaa	242
	Reverse	catagtgccaaggcctggtg	
<i>FN1</i>	Forward	accaacctacggatgactcg	230
	Reverse	gctcatctctggcatttt	
<i>PTX3</i>	Forward	gtgggtggagaggaacaaa	175
	Reverse	ttctcctctcaggacaatg	
<i>LGALS1</i>	Forward	ctctcgggtggagttctctg	158
	Reverse	acgaagctcttagcgtcagg	

Table 2. Genes with Upregulated mRNA Expression in KM12SM Cells Directly Cocultured with MSCs

Gene Name	KM12SM Alone (Normalized Cy5 Intensity)	KM12SM + MSCs Direct Coculture (Normalized Cy3 Intensity)
<i>SPARC</i>	6	636
<i>PTX3</i>	6	140
<i>FN1</i>	17	371
<i>FSTL1</i>	16	146
<i>LGALS1</i>	31	270

Immunofluorescence Staining of Frozen Sections and Formalin-Fixed Sections

Transplanted tumor tissues were prepared into 10-mm frozen sections and were then subjected to immunofluorescence analyses. The procedures for immunofluorescent staining of frozen sections were described previously [7]. For immunofluorescent staining of surgical specimens, formalin-fixed, paraffin-embedded tissues cut into serial 4-mm sections were treated with an Opal Fluorescent IHC Kit (Perkin Elmer, Norwalk, CT) according to the manufacturer's instructions. Primary antibodies used included goat polyclonal anti-fibronectin antibody and rabbit polyclonal anti-E-cadherin (Santa Cruz Biotechnology, Santa Cruz, CA). The fluorescent signal of secondary antibody was captured by confocal laser-scanning microscopy (Carl Zeiss Microscopy, Thornwood, NY).

Chamber Slides System

To evaluate the localization of FN expression in KM12SM cells cultured alone, KM12SM cells were seeded into a chamber slide system with DMEM supplemented with 0.5% FBS. After 48 hours of incubation, cells were rinsed with PBS and fixed with 4% paraformaldehyde for immunofluorescence staining.

To evaluate the localization of FN expression in KM12SM cells cocultured with MSCs-CM, KM12SM cells were seeded into a chamber slide system with DMEM supplemented with 0.5% FBS with MSC-CM. After 48 hours of incubation, cells were rinsed with

PBS and fixed with 4% paraformaldehyde for immunofluorescence staining.

To evaluate the localization of FN expression in KM12SM cells directly cocultured with MSCs, KM12SM cells and MSCs were seeded into a chamber slide system separately by cloning ring, and DMEM supplemented with 0.5% FBS was added. KM12SM cells were cultured inside the cloning ring, and MSCs were cultured outside the cloning ring. After 24 hours of incubation, the cloning ring was removed. After another 24 hours of incubation, cells were rinsed with PBS and fixed with 4% paraformaldehyde for immunofluorescence staining.

Immunofluorescence staining was performed using the Opal Fluorescent IHC Kit according to the manufacturer's protocol. Goat polyclonal anti-fibronectin antibody (Santa Cruz Biotechnology) was used as a primary antibody. The fluorescent signal of secondary antibody was captured by confocal laser-scanning microscopy (Carl Zeiss Microscopy).

Patients and Surgical Specimens

Archival formalin-fixed, paraffin-embedded tumor tissues were obtained from Hiroshima University Hospital. Specimens from 89 patients who underwent surgical resection for colon dysplasia and cancer were examined by immunohistochemistry. Patient privacy was protected in accordance with the Ethical Guidelines for Human Genome/Gene Research of the Japanese Government. All personally identifiable information was removed before analysis of the tissue samples.

Results

Direct Contact with MSCs Enhanced Proliferation and Migration of KM12SM Cells

We first examined the effect of MSCs on the proliferation and migration of KM12SM cells. KM12SM-GFP cells were cultured alone with fresh medium (control), with MSC-CM (indirect

Table 3. Comparison between Fibronectin-Positive and Fibronectin-Negative Cases of Dysplasia and Colorectal Carcinoma among Surgical Specimens

	FN Expression		P	
	Positive	Negative		
Number of patients	51	38		
Age (years old)	66.0 ± 11.7	68.2 ± 9.0	.25	
Median of observation period (year)	5	4.8	.41	
Location				
	Right side colon	15 (56%)	12	.98
	Left side colon	36 (58%)	26	
Morphological type				
	Depressed type	10 (56%)	8	.92
	Elevated type	41 (58%)	30	
Histological type (excluding unknown cases)				
	tub1	40 (54%)	34	.95
	tub2	4 (50%)	4	
Degree of progression (dysplasia vs SM or Adv Ca)				
	Dysplasia	10 (26%)	29	.0027*
	SM or Adv Ca	40 (82%)	9	
INF (excluding unknown cases)				
	a	4 (36%)	7	.48
	b or c	18 (55%)	15	
Quantity of stroma (excluding unknown cases)				
	Med	4 (57%)	3	.66
	Int or Sci	18 (69%)	8	
Lymphatic and/or blood vessel invasion				
	Yes	16 (80%)	4	.022*
	No	35 (51%)	33	
Lymph node metastasis				
	Yes	11 (92%)	1	.011*
	No	40 (52%)	37	
Other organ metastasis				
	Yes	4 (100%)	0	.13
	No	47 (55%)	38	

SM, submucosal invasive carcinoma; Adv Ca, advanced carcinoma; Med, medullary; Int, intermediate; Sci, scirrhous.

*P < .05.

Table 4. Comparison between Fibronectin-Positive and Fibronectin-Negative Cases of Submucosal Invasive Colorectal Carcinoma among Surgical Specimens

		FN expression		P
		Positive	Negative	
Number of patients		28	16	
Age (years old)		68.0 ± 11.7	70.9 ± 12.5	.24
Median of observation period (year)		5.2	4.7	.80
Location	Right side colon	8 (57%)	6	.78
	Left side colon	20 (43%)	10	
Morphological type	Depressed type	6 (55%)	5	.71
	Elevated type	22 (67%)	11	
Histological type (excluding unknown cases)	tub1	18 (64%)	10	.91
	tub2	8 (57%)	6	
Depth of SM invasion (µm)	2657 ± 1889	2365 ± 2028	0.39	
INF (excluding unknown cases)	a	2 (100%)	0	.60
	b or c	9 (53%)	8	
Quantity of stroma (excluding unknown cases)	Med	2 (40%)	3	.71
	Int or Sci	10 (63%)	6	
Lymphatic and/or blood vessel invasion	Yes	11 (78%)	3	.19
	No	17 (57%)	13	
Lymph node metastasis	Yes	9 (100%)	0	.031*
	No	19 (54%)	16	
Other organ metastasis	Yes	2 (100%)	0	.73
	No	26 (62%)	16	
Budding grade	Low	18 (56%)	14	.030*
	High	10 (83%)	2	

*P < .05.

coculture group), or with MSCs (direct coculture group). The proliferation and migration abilities of KM12SM cells were highest in the direct coculture group (Figure 1, A and B). The proliferation and

migration of KM12SM cells were not affected by coculture with MSC-CM (Figure 1, C and D), suggesting that direct cell-cell contact is necessary for enhancement of proliferation and migration.

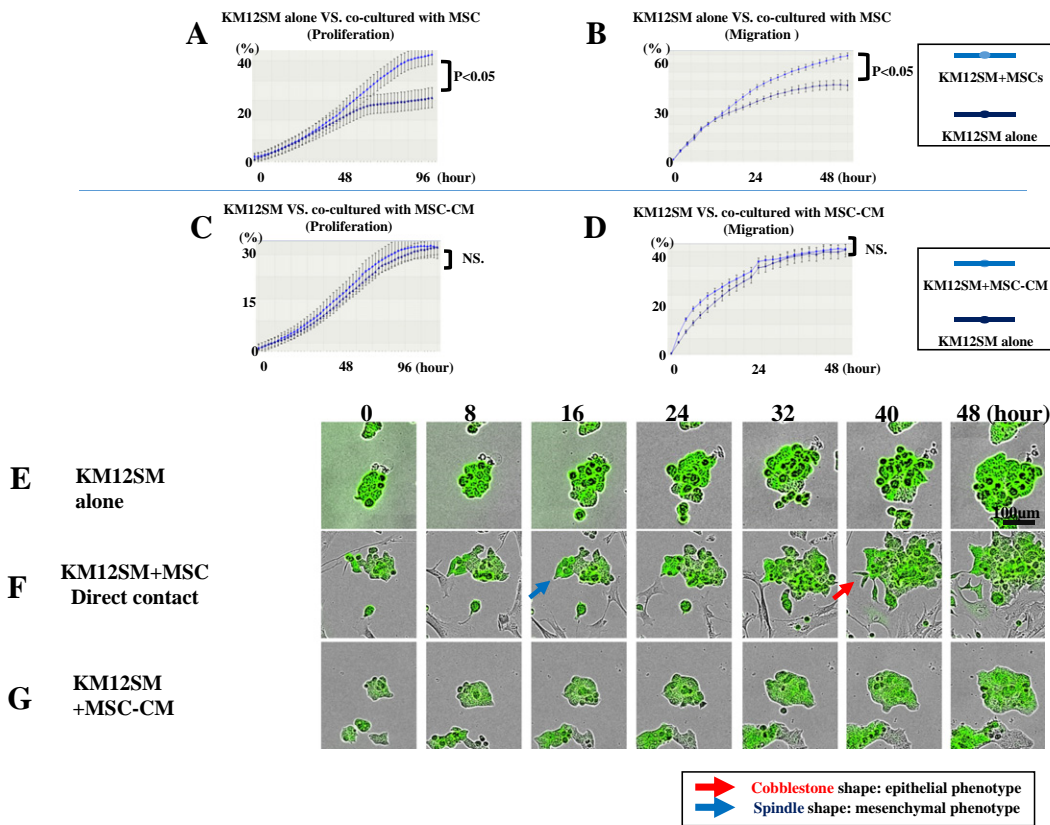


Figure 1. *In vitro* cell proliferation and migration of KM12SM cells. (A) Proliferation and (B) migration abilities of KM12SM cells cocultured with MSCs compared with those of KM12SM cells cultured alone. (C) Proliferation and (D) migration abilities of KM12SM cells cocultured with MSC-CM (indirect coculture) compared with those of KM12SM cells cultured alone. Time-lapse imaging (obtained with IncuCyte Zoom) of morphology of KM12SM cells cultured (E) alone, (F) with MSCs, or (G) with MSC-CM for 48 hours. Scale bar = 100 µm.

Morphological Changes and Movement of KM12SM Cells in Contact with MSCs

We next examined the effect of MSCs on the morphology of KM12SM cells. Time-lapse imaging was used to observe the morphology and movement of the cells. MSC-CM did not affect the morphology of KM12SM-GFP cells (Figure 1F). KM12SM-GFP cells directly attached to MSCs, however, exhibited a change in shape from cobblestone-like to spindle-like. These spindle-like cells were able to detach from tumor cell nests.

cDNA Microarray Analysis of KM12SM Colon Cancer Cells Cocultured with MSCs

To determine the genes involved in these phenomena, cDNA microarray analysis was performed using mRNAs extracted from each experimental group of KM12SM cells. Expression levels of secreted protein, acidic and rich in cysteine precursor (*SPARC*); pentraxin-related protein PTX3 precursor (*PTX3*); fibronectin precursor (*FN1*); follistatin-related protein 1 precursor (*FSTL1*); and galectin-1 (*LGALS1*) were higher in KM12SM cells directly cocultured with MSCs compared with levels in KM12SM cells cultured alone (Table 2 and Figure 2A). Validation of gene expression was performed by qRT-PCR (Figure 2B). Among these EMT-related genes, qRT-PCR analysis revealed that the *FN* gene was particularly upregulated when KM12SM cells were directly cocultured with MSCs. In contrast, expression of the above EMT-related genes was not significantly altered by indirect coculture with MSC-CM (Figure 2C).

FN Expression in KM12SM Cells Is Enhanced by Direct Contact with MSCs

Expression of FN was examined by time-lapse immunofluorescence at the cell level. KM12SM cells and MSCs were separately

cultured using cloning rings. After removal of the separating ring, cell-to-cell surface lesions between KM12SM cells and MSCs were observed by confocal laser-scanning microscopy. Strong FN expression was observed only in MSCs and at the edges of KM12SM cell clusters where KM12SM cells were in direct contact with MSCs (Figure 3A, lower panel). FN expression was not observed in KM12SM cells cultured alone or KM12SM cells cocultured with MSC-CM (Figure 3A, upper and middle panels).

Colocalization of FN Expression in Tumor-Bearing Mice after Injection of PKH26-GL-Labeled MSCs

After injection of PKH26-GL-labeled MSCs into the tail veins of KM12SM tumor-bearing mice, MSCs were detected selectively in the tumor stroma. Expression of FN was seen in the tumor stroma and at the edges of cancer nests where MSCs were in contact with cancer cells (Figure 3B).

Effect of MSC Coimplantation in Orthotopic Nude Mouse Model

In tumors generated by orthotopic implantation of KM12SM cells alone, expression of FN at the edges of cancer nests was relatively low, and E-cadherin expression in cancer nests was homogeneous. Marked EMT was not observed (Figure 3C). In contrast, in tumors generated by coimplantation of KM12SM cells and MSCs, expression of FN was seen not only in the tumor stroma but also at the edges of cancer nests in contact with the tumor stroma. Expression of E-cadherin was elevated in the centers of tumor nests but lower at the edges of cancer nests (Figure 3D). These results indicate that coimplantation of MSCs promotes EMT *in vivo* via direct contact between MSCs and cancer cells.

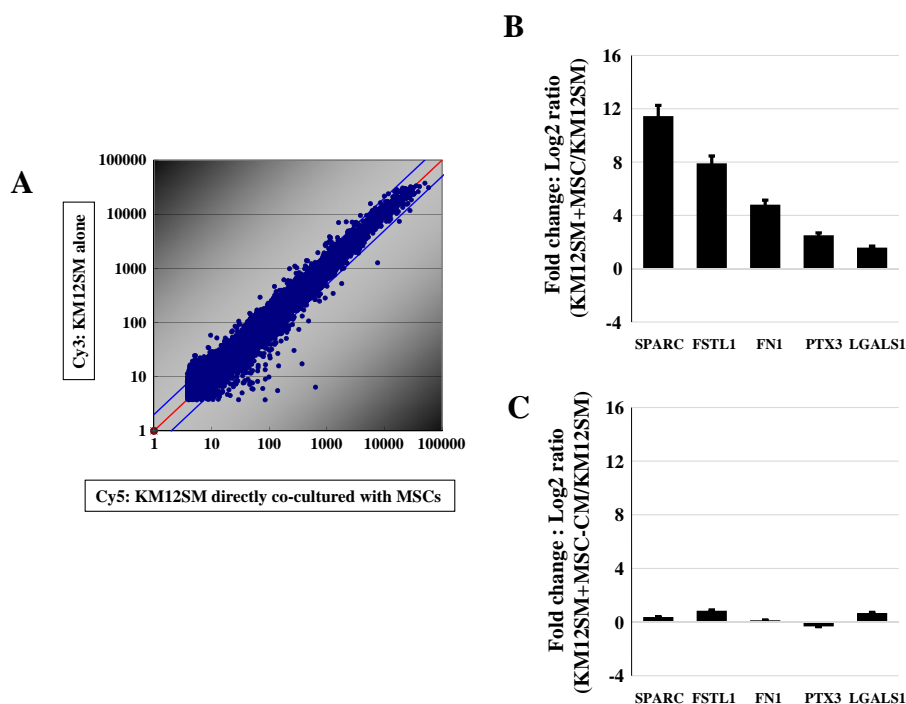


Figure 2. Microarray analysis of KM12SM cells. (A) Scatter plots for Cy5-labeled KM12SM cells (directly cocultured with MSCs) and Cy3-labeled KM12SM cells (cultured alone). (B) Expression of *SPARC*, *FSTL1*, *FN1*, *PTX3*, and *LGALS1* in KM12SM cells directly cocultured with MSCs versus expression in KM12SM cells cultured alone, as determined by qRT-PCR. (C) Expression of *SPARC*, *FSTL1*, *FN1*, *PTX3*, and *LGALS1* in KM12SM cells cocultured with MSC-CM versus expression in KM12SM cells cultured alone, as determined by qRT-PCR.

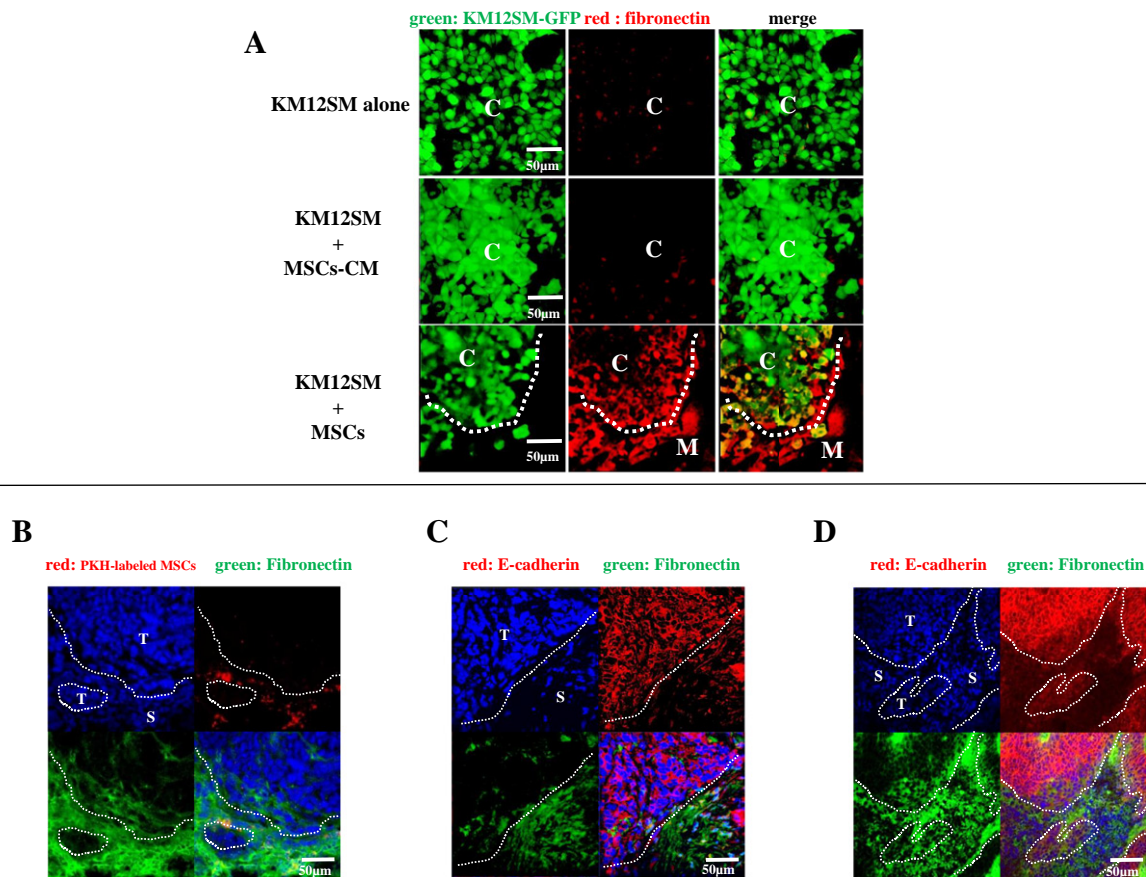


Figure 3. Immunofluorescence staining of KM12SM chamber slides and frozen sections obtained from orthotopic colon cancer models. (A) *In vitro* expression of FN (red) in KM12SM-GFP colon cancer cells (green) cultured alone (upper panels), with MSC-CM (middle panels), or with MSCs (lower panels). Merged images show regions of overlap. C, KM12SM cancer cells; M, MSCs. Scale bar = 50 μm. (B) Expression of FN (green) after injection of PKH26-GL-labeled MSCs (red) into the tail veins of KM12SM tumor-bearing mice. DAPI nuclear staining is shown in blue. Merged image shown in the lower right. T, tumor; S, stroma. Scale bar = 50 μm. (C) Expression of FN (green) and E-cadherin (red) in tumors generated by implantation of KM12SM cells only. DAPI nuclear staining is shown in blue. Merged image shown in the lower right. T, tumor; S, stroma. Scale bar = 50 μm. (D) Expression of FN (green) and E-cadherin (red) in tumors generated by coimplantation of KM12SM cells and MSCs. DAPI nuclear staining is shown in blue. Merged image shown in the lower right. T, tumor; S, stroma. Scale bar = 50 μm.

FN Expression in Surgical Specimens

To examine EMT localization, we performed immunostaining for FN in colorectal dysplasias and adenocarcinomas of surgical specimens. Degree of progression, as well as rates of lymphatic and vessel invasion and lymphatic metastasis, was higher in FN-positive patients than in FN-negative patients (Table 3). Subsequently, to evaluate the difference between FN-positive patients and FN-negative patients with similar depths of invasion, we analyzed the submucosal invasive adenocarcinomas and divided them into an FN-positive group and an FN-negative group. The characteristics of both groups are as shown in Table 4. There were no significant differences between the groups in patient age, tumor location, histological type, depth of submucosal invasion, infiltration (INF), quantity of stroma, or other organ metastasis. However, lymphatic invasion, metastasis, and budding grade were significantly higher in the FN-positive group (Table 4).

High expression of FN was seen not only in the stromal area but also at the invasive edges of cancer cells close to the stromal area (Figure 4A). In addition, expression of FN was seen in budding cells (Figure 4B). Furthermore, EMT was not observed in FN-negative or

low-budding grade patients, whereas EMT was active in FN-positive and high-budding grade patients (Figure 4C). Kaplan-Meier survival curves revealed that overall survival was significantly reduced in the FN-positive group compared with that in the FN-negative group (Figure 4D).

Discussion

EMT is a common process during wound healing and organ fibrosis in which epithelial cells undergo morphological changes resulting in increased cell plasticity and mobility as they transition into a mesenchymal-like cell phenotype. EMT can be also observed in a variety of cancer tissues. In human CRC, EMT is often detected at invasive lesions and tumor peripheries at the interface between cancer cells and host cells surrounded by extracellular matrix (ECM). EMT enhances the motility and invasion of tumor cells and thereby may result in metastasis.

In the present study, we demonstrated that direct contact between cancer cells and MSCs plays an important role in the induction of EMT in tumor cells. In culture, only tumor cells that are directly

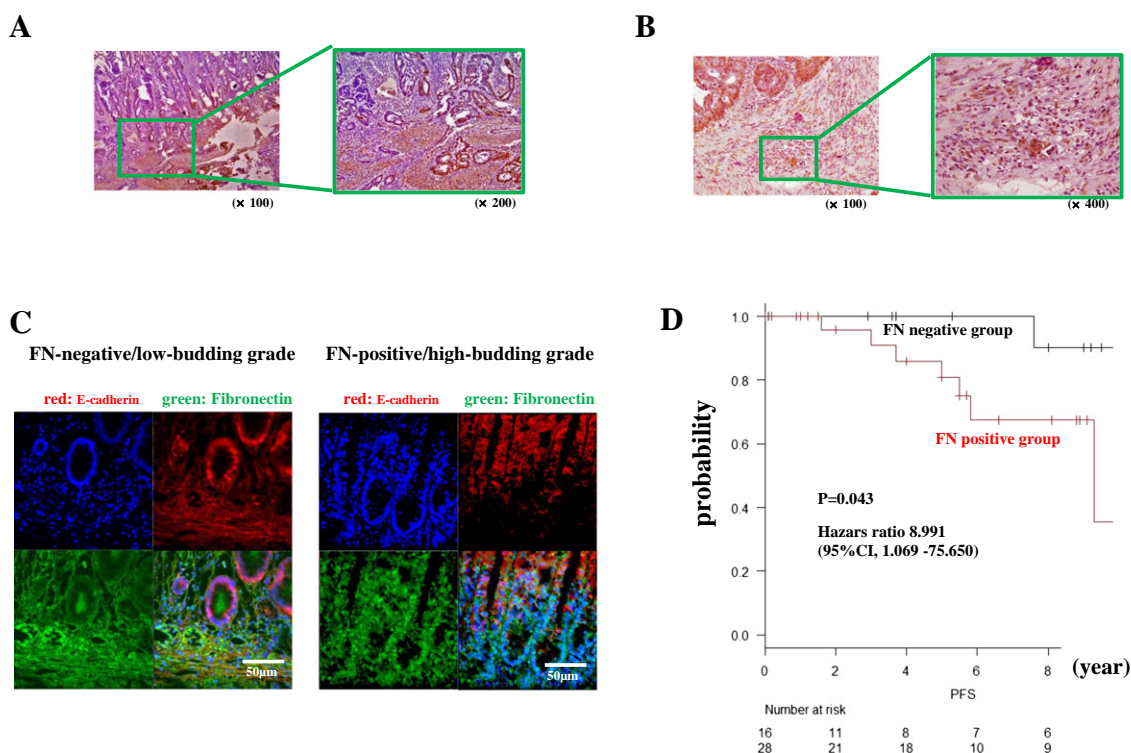


Figure 4. Expression of FN in surgical specimens of human colon tumors. (A) Expression of FN in the stromal area and at the invasive edges of cancer cells close to the stromal area. (B) Expression of FN in budding cells. (C) Expression of FN (green) and E-cadherin (red) in FN-negative/low-budding grade and FN-positive/high-budding grade patients. DAPI nuclear staining is shown in blue. Merged image shown in lower right. (D) Kaplan-Meier survival curves showing overall survival in FN-positive and FN-negative patient groups.

attached to MSCs showed morphological changes to mesenchymal-like cells. In contrast, no morphological changes were observed following the treatment of cancer cells with MSC-CM. Furthermore, microarray analysis showed that several genes involved in EMT were upregulated in tumor cells following direct coculture with MSCs. Pathway analysis also revealed enrichment for pathways related to matrix metalloproteinases (data not shown), which are well known EMT promoters [24]. Expression levels of *FN*, *SPARC*, *LGALS1*, *PTX3*, and *FSTL* were markedly upregulated in our microarray analysis. There are a few reports regarding the relationship between EMT and *PTX3/FSTL* [35,36], but it has not yet been elucidated how these affect EMT. *SPARC* is a matricellular protein known to be a marker of poor prognosis in different cancer types; it is involved in EMT, immune surveillance, and angiogenesis [37]. Furthermore, *SPARC* promotes migration activity in cancer cells [38]. It has been reported that *LGALS1* promotes EMT and that its expression correlates with cancer growth, invasiveness, and metastasis [39]. Among these upregulated genes, we focused on *FN* because it is a well-known EMT marker and EMT-promoting factor [40]. Thus far, it has been reported that cancer cells express soluble factors when interacting with MSCs and that these soluble factors promote tumor progression in a paracrine manner [41,42]. However, it has also been reported that MSCs affect cardiomyocytes via a juxtacrine signaling mechanism [43,44]. There have been a few reports that have revealed the importance of direct cell-to-cell contact in the cross talk between cancer cells and MSCs. These showed that MSCs interact with cancer cells by inducing cancer cells to shed amphiregulin via juxtacrine signaling [28]. We found that *FN* expression was induced only by direct contact with MSCs *in vitro* and

in vivo. We therefore present the novel findings that MSCs interact with cancer cells by cell-to-cell contact and that the interaction is mediated by EMT-related proteins such as *FN*. Other EMT-related genes that were significantly upregulated in our study, such as *SPARC* and galectin, are also of great interest. We speculate that these genes play a complementary role, such as enhancement of *FN* expression by *SPARC* [38]. The identification of genes with large effects as well as the mechanisms by which these genes interact to promote cancer progression remains subjects for future study.

The ECM is a key component of the cancer microenvironment and cooperates with other extracellular molecules to relay external signals into cells. *FN* is an ECM glycoprotein that plays roles in cell-substrate interactions, including cell adhesion, and appears to be important for differentiation and oncogenic transformation. Alteration of the ECM composition in cancer may be responsible for the tissue remodeling processes that are linked to cancer progression. Many reports have shown that expression of *FN* is upregulated in several cancer tissues, including colon cancer [45–48]. Furthermore, *FN* expression is reported to be absent from normal connective tissues, whereas increased *FN* expression levels have been detected in the tumor stroma [46,48].

FN is a well-known mesenchymal marker, and thus EMT increases *FN* expression. Park et al. reported that *FN* is not only an EMT marker but also a promoter of EMT [40]. They demonstrated that *FN* initiates EMT under serum-free conditions by enhancing the effect of endogenous *TGFβ*. They proposed that increased *FN* levels in breast cancer may be both a cause and an effect of tumor initiation and/or progression.

Tumor budding is defined by the presence of clusters of undifferentiated malignant cells in the tumor stroma located in close proximity ahead of the invasive front of a tumor [49–51]. Tumor budding has been reported to be an additional prognostic factor for colorectal carcinoma (CRC) according to the Union for International Cancer Control [52] and a potential prognostic factor in early CRC according to the European Society for Medical Oncology consensus guidelines [53]. Although evidence connecting tumor budding and EMT is scarce [54], some reports have indicated that EMT is significantly associated with tumor budding [55,56]. In our study, EMT was observed in budding cells, and tumor budding was promoted by the interaction between MSCs and the tumor stroma. Moreover, EMT accompanied by FN expression correlated with tumor budding and tumor progression.

In conclusion, MSCs induce EMT in colon cancer cells via direct cell-to-cell contact and are associated with colon cancer metastasis. Understanding the molecular mechanisms of this interaction between tumor cells and MSCs may lead to the establishment of new therapies targeting the tumor stroma.

Disclosure Statement

The authors have no conflict of interest.

Acknowledgements

This work was carried out with the kind cooperation of the Analysis Center of Life Science, Natural Science Center for Basic Research and Development, Hiroshima University. We would like to thank Editage (www.editage.jp) for English language editing.

References

- Jemal A, Bray F, Center MM, Ferlay J, Ward E, and Forman D (2011). Global cancer statistics. *CA Cancer J Clin* **61**, 69–90.
- Mantovani A, Allavena P, Sica A, and Balkwill F (2008). Cancer-related inflammation. *Nature* **454**, 436–444.
- Whiteside TL (2008). The tumor microenvironment and its role in promoting tumor growth. *Oncogene* **27**, 5904–5912.
- Kitadai Y, Sasaki T, Kuwai T, Nakamura T, Bucana CD, and Fidler IJ (2006). Targeting the expression of platelet-derived growth factor receptor by reactive stroma inhibits growth and metastasis of human colon carcinoma. *Am J Pathol* **169**, 2054–2065.
- Orimo A, Gupta PB, Sgroi DC, Arenzana-Seisdedos F, Delaunay T, Naeem R, Carey VJ, Richardson AL, and Weinberg RA (2005). Stromal fibroblasts present in invasive human breast carcinomas promote tumor growth and angiogenesis through elevated SDF-1/CXCL12 secretion. *Cell* **121**, 335–348.
- Kitadai Y, Sasaki T, Kuwai T, Nakamura T, Bucana CD, Hamilton SR, and Fidler IJ (2006). Expression of activated platelet-derived growth factor receptor in stromal cells of human colon carcinomas is associated with metastatic potential. *Int J Cancer* **119**, 2567–2574.
- Shinagawa K, Kitadai Y, Tanaka M, Sumida T, Kodama M, Higashi Y, Tanaka S, Yasui W, and Chayama K (2010). Mesenchymal stem cells enhance growth and metastasis of colon cancer. *Int J Cancer* **127**, 2323–2333.
- Takigawa H, Kitadai Y, Shinagawa K, Yuge R, Higashi Y, Tanaka S, Yasui W, and Chayama K (2016). Multikinase inhibitor regorafenib inhibits the growth and metastasis of colon cancer with abundant stroma. *Cancer Sci*.
- Studený M, Marini FC, Champlin RE, Zompetta C, Fidler IJ, and Andreeff M (2002). Bone marrow-derived mesenchymal stem cells as vehicles for interferon-beta delivery into tumors. *Cancer Res* **62**, 3603–3608.
- Kidd S, Caldwell L, Dietrich M, Samudio I, Spaeth EL, Watson K, Shi Y, Abbruzzese J, Konopleva M, and Andreeff M, et al (2010). Mesenchymal stromal cells alone or expressing interferon-beta suppress pancreatic tumors in vivo, an effect countered by anti-inflammatory treatment. *Cytotherapy* **12**, 615–625.
- Chen X, Lin X, Zhao J, Shi W, Zhang H, Wang Y, Kan B, Du L, Wang B, and Wei Y, et al (2008). A tumor-selective biotherapy with prolonged impact on established metastases based on cytokine gene-engineered MSCs. *Mol Ther* **16**, 749–756.
- Ren C, Kumar S, Chanda D, Chen J, Mountz JD, and Ponnazhagan S (2008). Therapeutic potential of mesenchymal stem cells producing interferon-alpha in a mouse melanoma lung metastasis model. *Stem Cells* **26**, 2332–2338.
- Li X, Lu Y, Huang W, Xu H, Chen X, Geng Q, Fan H, Tan Y, Xue G, and Jiang X (2006). In vitro effect of adenovirus-mediated human gamma interferon gene transfer into human mesenchymal stem cells for chronic myelogenous leukemia. *Hematol Oncol* **24**, 151–158.
- Nakamura K, Ito Y, Kawano Y, Kurozumi K, Kobune M, Tsuda H, Bizen A, Honmou O, Niitsu Y, and Hamada H (2004). Antitumor effect of genetically engineered mesenchymal stem cells in a rat glioma model. *Gene Ther* **11**, 1155–1164.
- Kanehira M, Xin H, Hoshino K, Maemondo M, Mizuguchi H, Hayakawa T, Matsumoto K, Nakamura T, Nukiwa T, and Saijo Y (2007). Targeted delivery of NK4 to multiple lung tumors by bone marrow-derived mesenchymal stem cells. *Cancer Gene Ther* **14**, 894–903.
- Loebinger MR, Kyrtatos PG, Turmaine M, Price AN, Pankhurst Q, Lythgoe MF, and Janes SM (2009). Magnetic resonance imaging of mesenchymal stem cells homing to pulmonary metastases using biocompatible magnetic nanoparticles. *Cancer Res* **69**, 8862–8867.
- Sasportas LS, Kasmieh R, Wakimoto H, Hingtgen S, van de Water JA, Mohapatra G, Figueiredo JL, Martuza RL, Weissleder R, and Shah K (2009). Assessment of therapeutic efficacy and fate of engineered human mesenchymal stem cells for cancer therapy. *Proc Natl Acad Sci U S A* **106**, 4822–4827.
- Grisendi G, Bussolari R, Cafarelli L, Petak I, Rasini V, Veronesi E, De Santis G, Spano C, Tagliazzucchi M, and Barti-Juhasz H, et al (2010). Adipose-derived mesenchymal stem cells as stable source of tumor necrosis factor-related apoptosis-inducing ligand delivery for cancer therapy. *Cancer Res* **70**, 3718–3729.
- Baksh D, Song L, and Tuan RS (2004). Adult mesenchymal stem cells: characterization, differentiation, and application in cell and gene therapy. *J Cell Mol Med* **8**, 301–316.
- Feldmann Jr RE, Bieback K, Maurer MH, Kalenka A, Burgers HF, Gross B, Hunzinger C, Kluter H, Kuschinsky W, and Eichler H (2005). Stem cell proteomes: a profile of human mesenchymal stem cells derived from umbilical cord blood. *Electrophoresis* **26**, 2749–2758.
- Iacobuzio-Donahue CA, Argani P, Hempen PM, Jones J, and Kern SE (2002). The desmoplastic response to infiltrating breast carcinoma: gene expression at the site of primary invasion and implications for comparisons between tumor types. *Cancer Res* **62**, 5351–5357.
- Parham DM (2001). Pathologic classification of rhabdomyosarcomas and correlations with molecular studies. *Mod Pathol* **14**, 506–514.
- Karnoub AE, Dash AB, Vo AP, Sullivan A, Brooks MW, Bell GW, Richardson AL, Polyak K, Tubo R, and Weinberg RA, et al (2007). Mesenchymal stem cells within tumour stroma promote breast cancer metastasis. *Nature* **449**, 557–563.
- Chu YJ, Tang HJ, Guo Y, Guo J, Huang BX, Fang F, Cai J, and Wang ZH (2015). Adipose-derived mesenchymal stem cells promote cell proliferation and invasion of epithelial ovarian cancer. *Exp Cell Res* **337**, 16–27.
- Thomas C and Karnoub AE (2013). Lysyl oxidase at the crossroads of mesenchymal stem cells and epithelial-mesenchymal transition. *Oncotarget* **4**, 376–377.
- Tanabe S, Aoyagi K, Yokozaki H, and Sasaki H (2015). Regulated genes in mesenchymal stem cells and gastric cancer. *World J Stem Cells* **7**, 208–222.
- Wang ML, Pan CM, Chiou SH, Chen WH, Chang HY, Lee OK, Hsu HS, and Wu CW (2012). Oncostatin m modulates the mesenchymal-epithelial transition of lung adenocarcinoma cells by a mesenchymal stem cell-mediated paracrine effect. *Cancer Res* **72**, 6051–6064.
- Carnet O, Lecomte J, Masset A, Primac I, Durre T, Maertens L, Detry B, Blacher S, Gilles C, and Pequeux C, et al (2015). Mesenchymal stem cells shed amphiregulin at the surface of lung carcinoma cells in a juxtacrine manner. *Neoplasia* **17**, 552–563.
- Morikawa K, Walker SM, Nakajima M, Pathak S, Jessup JM, and Fidler IJ (1988). Influence of organ environment on the growth, selection, and metastasis of human colon carcinoma cells in nude mice. *Cancer Res* **48**, 6863–6871.
- Ishii M, Koike C, Igarashi A, Yamanaka K, Pan H, Higashi Y, Kawaguchi H, Sugiyama M, Kamata N, and Iwata T, et al (2005). Molecular markers distinguish bone marrow mesenchymal stem cells from fibroblasts. *Biochem Biophys Res Commun* **332**, 297–303.

- [31] Tsutsumi S, Shimazu A, Miyazaki K, Pan H, Koike C, Yoshida E, Takagishi K, and Kato Y (2001). Retention of multilineage differentiation potential of mesenchymal cells during proliferation in response to FGF. *Biochem Biophys Res Commun* **288**, 413–419.
- [32] Liu L, Wang YD, Wu J, Cui J, and Chen T (2012). Carnitine palmitoyltransferase 1A (CPT1A): a transcriptional target of PAX3-FKHR and mediates PAX3-FKHR-dependent motility in alveolar rhabdomyosarcoma cells. *BMC Cancer* **12**, 154.
- [33] Shinagawa K, Kitadai Y, Tanaka M, Sumida T, Onoyama M, Ohnishi M, Ohara E, Higashi Y, Tanaka S, and Yasui W, et al (2013). Stroma-directed imatinib therapy impairs the tumor-promoting effect of bone marrow-derived mesenchymal stem cells in an orthotopic transplantation model of colon cancer. *Int J Cancer* **132**, 813–823.
- [34] Sumida T, Kitadai Y, Shinagawa K, Tanaka M, Kodama M, Ohnishi M, Ohara E, Tanaka S, Yasui W, and Chayama K (2011). Anti-stromal therapy with imatinib inhibits growth and metastasis of gastric carcinoma in an orthotopic nude mouse model. *Int J Cancer* **128**, 2050–2062.
- [35] Scimeca M, Antonacci C, Colombo D, Bonfiglio R, Buonomo OC, and Bonanno E (2016). Emerging prognostic markers related to mesenchymal characteristics of poorly differentiated breast cancers. *Tumour Biol* **37**, 5427–5435.
- [36] Nogai H, Rosowski M, Grun J, Rietz A, Debus N, Schmidt G, Lauster C, Janitz M, Vortkamp A, and Lauster R (2008). Follistatin antagonizes transforming growth factor-beta3-induced epithelial-mesenchymal transition in vitro: implications for murine palatal development supported by microarray analysis. *Differentiation* **76**, 404–416.
- [37] Podhajcer OL, Benedetti LG, Girotti MR, Prada F, Salvatierra E, and Llera AS (2008). The role of the matricellular protein SPARC in the dynamic interaction between the tumor and the host. *Cancer Metastasis Rev* **27**, 691–705.
- [38] Yusuf N, Inagaki T, Kusunoki S, Okabe H, Yamada I, Matsumoto A, Terao Y, Takeda S, and Kato K (2014). SPARC was overexpressed in human endometrial cancer stem-like cells and promoted migration activity. *Gynecol Oncol* **134**, 356–363.
- [39] Manzi M, Bacigalupo ML, Carabias P, Elola MT, Wolfenstein-Todel C, Rabinovich GA, Espelt MV, and Troncoso MF (2016). Galectin-1 controls the proliferation and migration of liver sinusoidal endothelial cells and their interaction with hepatocarcinoma cells. *J Cell Physiol* **231**, 1522–1533.
- [40] Park J and Schwarzbauer JE (2014). Mammary epithelial cell interactions with fibronectin stimulate epithelial-mesenchymal transition. *Oncogene* **33**, 1649–1657.
- [41] Spaeth EL, Dembinski JL, Sasser AK, Watson K, Klopp A, Hall B, Andreeff M, and Marini F (2009). Mesenchymal stem cell transition to tumor-associated fibroblasts contributes to fibrovascular network expansion and tumor progression. *PLoS One* **4**, e4992.
- [42] El-Haibi CP and Karnoub AE (2010). Mesenchymal stem cells in the pathogenesis and therapy of breast cancer. *J Mammary Gland Biol Neoplasia* **15**, 399–409.
- [43] Sassoli C, Pini A, Mazzanti B, Quercioli F, Nistri S, Saccardi R, Zecchi-Orlandini S, Bani D, and Formigli L (2011). Mesenchymal stromal cells affect cardiomyocyte growth through juxtacrine Notch-1/Jagged-1 signaling and paracrine mechanisms: clues for cardiac regeneration. *J Mol Cell Cardiol* **51**, 399–408.
- [44] Rahbarghazi R, Nassiri SM, Khazrainia P, Kajbafzadeh AM, Ahmadi SH, Mohammadi E, Molazem M, and Zamani-Ahmadmhamudi M (2013). Juxtacrine and paracrine interactions of rat marrow-derived mesenchymal stem cells, muscle-derived satellite cells, and neonatal cardiomyocytes with endothelial cells in angiogenesis dynamics. *Stem Cells Dev* **22**, 855–865.
- [45] Loridon-Rosa B, Vielh P, Cuadrado C, and Burtin P (1988). Comparative distribution of fibronectin and vitronectin in human breast and colon carcinomas. An immunofluorescence study. *Am J Clin Pathol* **90**, 7–16.
- [46] Hauptmann S, Zardi L, Siri A, Carnemolla B, Borsi L, Castellucci M, Klosterhalfen B, Hartung P, Weis J, and Stocker G, et al (1995). Extracellular matrix proteins in colorectal carcinomas. Expression of tenascin and fibronectin isoforms. *Lab Invest* **73**, 172–182.
- [47] Inufusa H, Nakamura M, Adachi T, Nakatani Y, Shindo K, Yasutomi M, and Matsuura H (1995). Localization of oncofetal and normal fibronectin in colorectal cancer. Correlation with histologic grade, liver metastasis, and prognosis. *Cancer* **75**, 2802–2808.
- [48] Pujuguet P, Hammann A, Moutet M, Samuel JL, Martin F, and Martin M (1996). Expression of fibronectin ED-A+ and ED-B+ isoforms by human and experimental colorectal cancer. Contribution of cancer cells and tumor-associated myofibroblasts. *Am J Pathol* **148**, 579–592.
- [49] De Smedt L, Palmans S, and Sagaert X (2016). Tumour budding in colorectal cancer: what do we know and what can we do? *Virchows Arch* **468**, 397–408.
- [50] Koelzer VH, Zlobec I, and Lugli A (2016). Tumor budding in colorectal cancer—ready for diagnostic practice? *Hum Pathol* **47**, 4–19.
- [51] van Wyk HC, Park J, Roxburgh C, Horgan P, Foulis A, and DC McMillan (2015). The role of tumour budding in predicting survival in patients with primary operable colorectal cancer: a systematic review. *Cancer Treat Rev* **41**, 151–159.
- [52] Gospodarowicz MK, O'Sullivan B, and Sobin LH (2006). Prognostic factors in cancer, vol. Wiley-Liss Frankfurt; 2006 .
- [53] Schmoll H, Van Cutsem E, Stein A, Valentini V, Glimelius B, Haustermans K, Nordlinger B, Van de Velde C, Balmana J, and Regula J (2012). ESMO consensus guidelines for management of patients with colon and rectal cancer. A personalized approach to clinical decision making. *Ann Oncol* **23**, 2479–2516.
- [54] Grigore AD, Jolly MK, Jia D, Farach-Carson MC, and Levine H (2016). Tumor budding: the name is EMT. Partial EMT. *J Clin Med* **5**, 51.
- [55] Niwa Y, Yamada S, Koike M, Kanda M, Fujii T, Nakayama G, Sugimoto H, Nomoto S, Fujiwara M, and Kodera Y (2014). Epithelial to mesenchymal transition correlates with tumor budding and predicts prognosis in esophageal squamous cell carcinoma. *J Surg Oncol* **110**, 764–769.
- [56] Masugi Y, Yamazaki K, Hibi T, Aiura K, Kitagawa Y, and Sakamoto M (2010). Solitary cell infiltration is a novel indicator of poor prognosis and epithelial-mesenchymal transition in pancreatic cancer. *Hum Pathol* **41**, 1061–1068.